

# Pull-out behavior of headed anchors used in a totally prefabricated counterfort retaining wall system

Maen Farhat, Mohsen Issa, and Bruno F. J. Prado

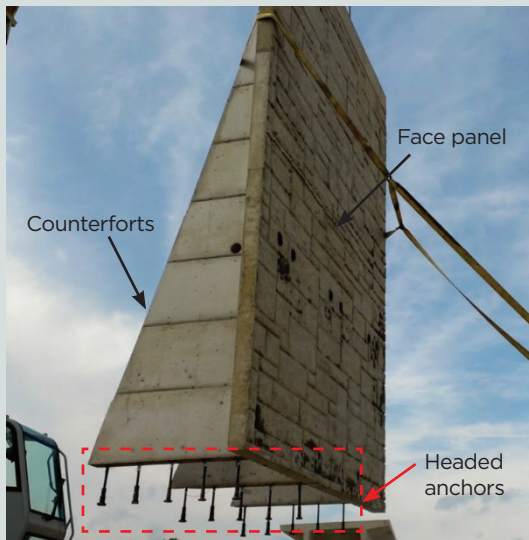
- This paper studies the pull-out behavior of headed anchors used in a totally prefabricated counterfort retaining wall system through an experimental testing program as well as finite element analysis.
- The testing program included various anchor bar sizes and embedment lengths and studied the mode of failure when subjected to tensile loading.
- Results of the test program were compared with results from various design methods, including those from the American Concrete Institute, the American Institute of Steel Construction, and the American Society of Civil Engineers.

**A** totally prefabricated counterfort retaining wall system was developed as a method for fast-track construction. It is composed of a precast concrete base slab and a precast concrete face panel with three counterforts that are connected on-site with headed anchors. In this study, an experimental testing program was conducted to examine the pull-out behavior of the headed anchors. The study took into account different bar sizes, ranging from 19M to 29M (no. 6 to 9), that can be used in the design process, as well as two different commercially available grout types and headed anchors. The anchors were studied with different embedded lengths to examine the change in the mode of failure associated with changing the embedment depth of the headed anchors. In addition, a detailed three-dimensional finite element analysis was performed to further investigate the damage development in the anchors and shear pocket under axial loading conditions. The model was calibrated using the results obtained from the experimental testing. Finally, the results obtained from the experimental testing and finite element analysis were compared with the results obtained from the different design methods.

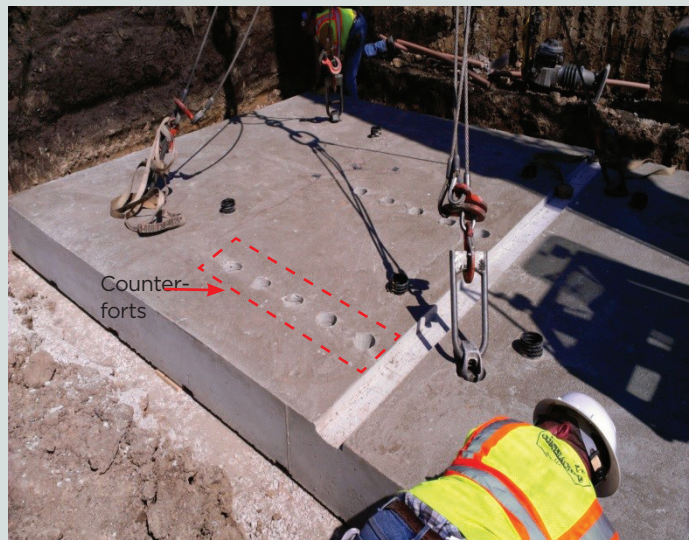
*PCI Journal* (ISSN 0887-9672) V. 64, No. 1, January–February 2019.

*PCI Journal* is published bimonthly by the Precast/Prestressed Concrete Institute, 200 W. Adams St., Suite 2100, Chicago, IL 60606.

Copyright © 2019, Precast/Prestressed Concrete Institute. The Precast/Prestressed Concrete Institute is not responsible for statements made by authors of papers in *PCI Journal*. Original manuscripts and letters on published papers are accepted on review in accordance with the Precast/Prestressed Concrete Institute's peer-review process. No payment is offered.



Counterfort wall component



Precast concrete base slab component

**Figure 1.** Components of totally prefabricated counterfort retaining wall: counterfort wall with headed anchors and base slab.

## System development

In the totally prefabricated counterfort retaining wall system, the face panel and the counterforts act as one component because they are connected with headed anchors. The headed anchors extend from the bottom of the counterforts and are placed in truncated shear pockets designed in the base slab. The anchors are grouted in the base slab to develop full composite action between the counterforts and the base slab.

According to a study by Farhat et al.,<sup>1-3</sup> a 6.15 m (20.18 ft) high, 3.96 m (12.99 ft) wide, full-scale prototype was designed according to the provisions given in the American Association of State Highway and Transportation Officials' *AASHTO LRFD Bridge Design Specifications*.<sup>4</sup> The prototype was optimized, fabricated, instrumented, and experimentally tested against soil backfill load, surcharge load, and an additional applied load of 871.8 kN (196 kip) using hydraulic actuators. The headed anchors play the most important role in maintaining the integrity of the system and ensuring the full composite action between the base slab and the wall component. **Figures 1** and **2** show the components and final assembly of the proposed system, respectively.

The main results of the study can be summarized as follows:

- The system experienced a very small deflection of 5 mm (0.2 in.) at its middle.
- Headed anchors showed excellent performance in maintaining the composite action between the precast concrete wall and the base slab at service and ultimate loads.
- The design of headed anchors is controlled by the outermost anchors, and a smaller bar size can be used for anchors close to the face panel because they experience



Front elevation



Rear elevation

**Figure 2.** Final assembly of totally prefabricated counterfort retaining wall showing front and rear elevations.

smaller tensile strain. In addition, the strain readings in the main reinforcing steel of the counterforts showed that the counterforts resist the entire applied lateral load. Therefore, two assumptions can be made by the designer:

- The headed anchors should be properly designed to resist the entire applied bending moment and shear forces.
- The main reinforcing steel in the counterforts should be designed to resist the entire lateral load, assuming that the bottom of the counterforts is fully bonded to the base slab.

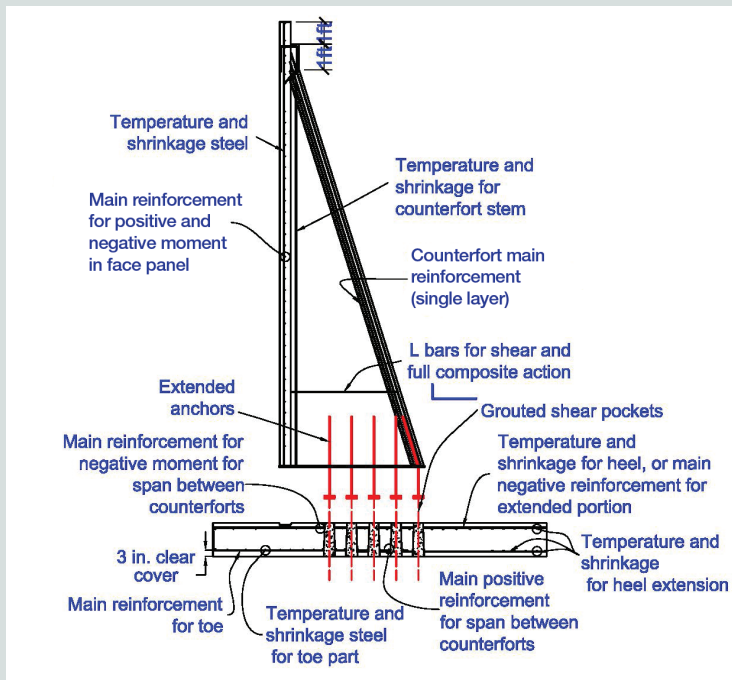
A study by Farhat and Issa<sup>5</sup> outlined the fabrication and construction procedures of the proposed system. The shear pocket is a tapered cylinder with top and bottom diameters of 127 and 152 mm (5 and 6 in.), respectively, and a depth equal to the depth of the slab. Upon placement of the upper wall component, the headed anchors are aligned inside the shear pocket and fast-setting grout is used to enforce the bond between the components.

The shear pockets are formed during the fabrication of the base slab by means of truncated cylinders wrapped with debonding agent. After concrete setting, the truncated cylinders are removed from the base slab to create the desired shear pocket. **Figure 3** shows the general assembly of the proposed system, the truncated cylinder wrapped with debonding agent, the headed anchors used to connect the precast concrete systems, and a cross section of the shear pocket.

Another study by Farhat and Issa<sup>6</sup> outlined the design process of the proposed system. The lateral loads applied to the proposed retaining wall system include lateral soil pressure and live surcharge load. These loads result in overturning moment at the bottom of the counterforts. The headed

anchors are designed to resist the entire applied overturning moment in the form of axial tension (**Fig. 4**). In particular, the anchors are designed to yield before breakout in concrete. However, under axial tensile loads, the load-carrying capacity of the headed anchors is controlled by the mode of failure anticipated at the anchor-shear pocket level. The mode of failure can be either fracture in steel, grout frictional pull-out, or concrete conical breakout.<sup>7</sup> Therefore, insufficient knowledge of the actual mode of failure may result in a difference between the design assumptions and the actual structural performance.

Full-scale experimental testing was conducted to assess the overall structural behavior of the system. However, additional



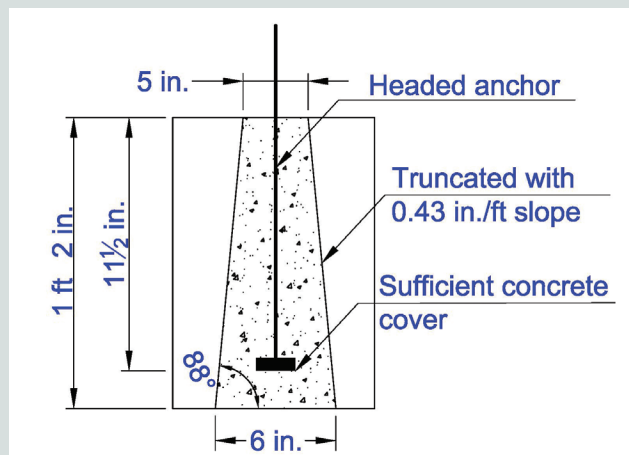
Components of proposed wall



Tapered concrete cylinder with debonding agent



Two types of available headed anchors



Details for truncated shear pocket

**Figure 3.** Components and anchor details for typical construction of the proposed wall. Note: 1 in. = 25.4 mm; 1 ft = 0.305 m.

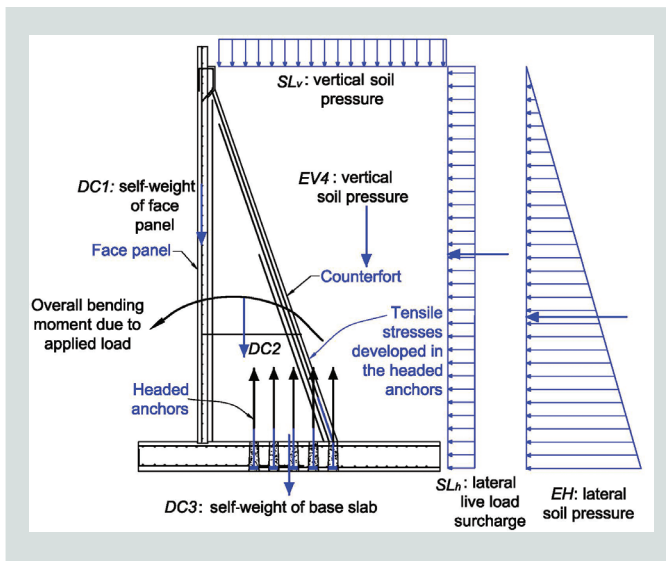


**Figure 4.** Load-resistance behavior of headed anchors under applied load.

investigation of the behavior of the headed anchors at the level of the grouted shear pockets is required.

## Background

Few studies in the literature have been conducted on large headed bars subjected to pull-out load. Most of the studies focused on the pull-out behavior of small shear studs at a shallow depth.<sup>8–15</sup> Lee et al.<sup>16</sup> conducted experimental testing on large headed anchors (diameter greater than 50.8 mm [2 in.]) and large embedment depths in concrete (greater than 635 mm [25 in.]). The objective of the testing was to investigate the anchors' suitability for use in nuclear power plants. The authors showed that the breakout cone with the concrete surface varied from 20 to 30 degrees.

According to the provisions given in chapter 17 of the American Concrete Institute's (ACI's) *Building Code Requirements for Structural Concrete (ACI 318-14) and Commentary (ACI 318R-14)*,<sup>7</sup> the tensile capacity of a headed anchor is controlled either by the nominal strength of an anchor in tension (section 17.4.1.2) or by the concrete breakout strength of an anchor in tension (section 17.4.2). The nominal strength of the anchor in tension  $N_{sa}$  shall not exceed  $A_{se,N}f_{uta}$  (section 17.4.1.2), where  $A_{se,N}$  is the effective cross-sectional area of the anchor bar. The specified tensile strength of anchor steel  $f_{uta}$  shall not be taken greater than the smaller of  $1.9f_{ya}$  and 861.8 MPa (125,000 psi), where  $f_{ya}$  is the specified yield strength of anchor steel.

The concrete capacity design method is used in the formulas adopted by ACI 318 for concrete breakout formulas. According to ACI 318-14, the average concrete breakout capacity of headed anchors in uncracked concrete is given by ACI 318-14 Eq. (17.4.2.1a). The basic concrete breakout strength of a single anchor in tension in cracked concrete is given by ACI 318-14 Eq. (17.4.2.2a), where  $k_c$  equals 24 for cast-in anchors and 17 for postinstalled anchors. The value of  $k_c$  is permitted to be between 17 and 24 for postinstalled anchors. The values

of  $k_c$  were determined from a large database of test results of uncracked concrete at the 5% fractile.<sup>7,17</sup> ACI 318-14 Eq. (17.4.2.2b) can be used for cast-in headed studs and headed bolts with  $279 \text{ mm} \leq h_{ef} \leq 635 \text{ mm}$  ( $11 \text{ in.} \leq h_{ef} \leq 25 \text{ in.}$ ). The concrete capacity design method presented in the American Institute of Steel Construction (AISC) steel design guide for base plate and anchor rods<sup>18</sup> is based on ACI 318. **Table 1** summarizes the concrete breakout/pull-out equations developed in different design methods and past literature.

DeVries<sup>19</sup> tested over 140 concrete blocks with headed reinforcing bars as part of an extensive study conducted by the University of Texas at Austin. The study assumed a value of 5 for the embedment depth-to-clear cover ratio for the shallow embedded tests and higher for the deep tests. The bearing strength and pull-out capacity of a single headed anchor were developed by FHWA/TX-04/1855-3 and DeVries (see Table 1 for equations). In the second phase of this project, Bashandy<sup>20</sup> conducted 14 pull-out tests. The purpose was to study the applicability of using plate-anchored bars as shear reinforcement under cyclic loading. It was found that the anchorage was not significantly affected in the first 15 cycles with a stress level of 5% to 80%.

Delhomme et al.<sup>21</sup> conducted pull-out tension tests on cast-in-place concrete blocks with a  $254 \times 254 \times 25.4 \text{ mm}$  ( $10 \times 10 \times 1 \text{ in.}$ ) plate welded to four ribbed bars or two headed studs. The study considered different bar sizes and embedment depths. It was found that headed anchors provide better ductility than bonded bars. It was also found that Eurocode 222 tends to underestimate the mean ultimate strength of the concrete breakout cone.

The damage process in engineered cementitious composites reinforced with fibers around headed anchors subjected to tensile load was examined using experimental testing and finite element analysis.<sup>23</sup> The study considered small headed anchors that were 8 mm (0.31 in.) in diameter with a 5 mm (0.196 in.) thick head, a 15 mm (0.59 in.) diameter head, and a 30 mm (1.18 in.) embedment depth. It was found using experimental testing that the ductility in the concrete due to fibers caused a change in the mode of failure of the pull-out headed anchors from brittle to ductile.

## Test specimens

The experimental testing program was conducted on 18 precast concrete blocks. The following parameters were considered:

- Type of headed anchor: Two types of commercially available headed anchors were used. The first type was labeled D and the second type was labeled P. **Table 2** shows the specifications and details for type D anchors. Type P has the same specifications as type D, but with a head thickness of 38 mm (1.5 in.). All bars were epoxy coated to consider the worst-case scenario.
- Size of headed anchor: 29M, 25M, 22M, and 19M (no. 9, 8, 7, and 6) headed anchors were considered.

**Table 1.** Breakout/pull-out equations in the design methods and past literature

Design method or literature reference and equation number, if applicable	Equation	Remark
AISC guide 1	$P = 0.85f'_c A_1 \sqrt{\frac{A_2}{A_1}}$	Concentric compressive axial load
AISC guide 1	$\phi N_p = 8\phi\psi_4 A_{brg} f'_c$	Concrete pull-out strength
AISC guide 1	$\phi N_{cgb} = \phi\psi_3 k_c \sqrt{f'_c} h_{ef}^{1.5} \frac{A_N}{A_{N0}}$	Concrete capacity design method
ACI 318-14 Eq. (17.4.2.1a)	$N_{cb} = \frac{A_{Nc}}{A_{Nco}} \psi_{ed,N} \psi_{c,N} \psi_{cp,N} N_b$	Nominal concrete (uncracked) breakout strength for single anchor
ACI 318-14 Eq. (17.4.2.2a)	$N_b = k_c \lambda_a \sqrt{f'_c} h_{ef}^{1.5}$	Basic concrete (cracked) breakout strength of a single anchor in tension.
ACI 318-14 Eq. (17.4.2.2b)	$N_b = 16\lambda_a \sqrt{f'_c} h_{ef}^{5/3}$	Cast-in headed studs and headed bolts with $279 \text{ mm} \leq h_{ef} \leq 635 \text{ mm}$
ACI 318-14 Eq. (17.4.3.1) and (17.4.3.4)	$N_{pn} = \psi_{c,P} N_p$ and $N_p = 8A_{brg} f'_c$	Pull-out strength of headed anchors
FHWA/TX-04/1855-3	$f_{s,head} = 2n_{5\%} \sqrt{\frac{A_{nh}}{A_b}} \left( \frac{c_1}{\sqrt{d_b}} \right) \psi f'_c$ $\psi = 0.6 + 0.4 \frac{c_2}{c_1}$	Bearing strength of headed anchors
DeVries	$P_u = \psi \frac{A_{bo}}{A_{bon}} \left( \frac{c_1 \sqrt{A_n f'_c}}{80} \right)$ $\psi = 0.7 + 0.3 \frac{c_2}{c_1}$	Pull-out strength of headed anchors

Note:  $A_1$  = loaded area for consideration of bearing strength;  $A_2$  = area of the lower base of the largest frustum of a pyramid, cone, or tapered wedge contained wholly;  $A_b$  = area of the bar or anchor;  $A_{bo}$  = blowout area for corner placement;  $A_{bon}$  = basic blowout area for corner placement;  $A_{brg}$  = bearing area of the anchor rod head or nut or net bearing area of the head of stud, anchor bolt, or headed deformed bar;  $A_N$  = Concrete breakout cone area for group;  $A_{N0}$  = Concrete breakout cone area for single anchor;  $A_{Nc}$  = projected concrete failure area of a single anchor or group of anchors;  $A_{Nco}$  = projected concrete failure area of a single anchor for calculation of strength in tension if not limited by edge distance or spacing;  $A_{nh}$  = net bearing area of the head (neglecting the bar area);  $c_1$  = dimension orthogonal to  $c_2$ ;  $c_2$  = the minimum of half the center-to-center bar spacing or the least overall cover dimension measured to the center of the bar;  $d_b$  = diameter of the bar or anchor;  $f'_c$  = concrete compressive strength;  $f_{s,head}$  = bearing strength of headed anchors;  $h_{ef}$  = effective embedment depth of anchor;  $k_c$  = coefficient for basic concrete breakout strength in tension;  $n_{5\%}$  = 5% exclusion factor;  $N_b$  = basic concrete (cracked) breakout strength of a single anchor in tension;  $N_{cb}$  = nominal concrete (uncracked) breakout strength of a single anchor;  $N_{cgb}$  = nominal concrete (uncracked) breakout strength of a single anchor calculated by the concrete capacity design method;  $N_p$  = nominal pull-out strength;  $N_{pn}$  = pull-out strength of headed anchors;  $P$  = nominal pull-out strength;  $\lambda_a$  = modification factor to reflect the reduced mechanical properties of lightweight concrete in certain concrete anchorage applications;  $\phi$  = strength reduction factor;  $\psi_3$  = factor used to modify pull-out strength of anchors based on presence or absence of cracks in concrete;  $\psi_4$  = factor used to modify concrete breakout strength of a single anchor based on presence or absence of cracks in concrete;  $\psi$  = radial disturbance factor;  $\psi_{c,N}$  = factor used to modify tensile strength of anchors based on presence or absence of cracks in concrete;  $\psi_{c,P}$  = factor used to modify pull-out strength of anchors based on presence or absence of cracks in concrete;  $\psi_{cp,N}$  = factor used to modify tensile strength of postinstalled anchors intended for use in uncracked concrete without supplementary reinforcement to account for the splitting tensile stresses due to installation;  $\psi_{ed,N}$  = factor used to modify tensile strength of anchors based on proximity to edges of concrete member. 1 mm = 0.0394 in.

**Table 2.** Specifications and details for type D headed anchors

	Bar diameter, mm	Head diameter, mm	Head thickness, mm	Ultimate pull-out strength $P_u$ , kN
19M	19.05	60.12	14.3	176.15
22M	22.23	70.21	15.88	240.2
25M	25.4	80.57	15.88	316.27
29M	28.65	90.65	17.48	400.34

Note: 19M = no. 6; 22M = no. 7; 25M = no. 8; 29M = no. 9; 1 mm = 0.0394 in.; 1 kN = 0.225 kip.

- Type of concrete grout: Two types of commercially available grout certified by the Illinois Department of Transportation (IDOT) were considered. The first type of proprietary grout was labeled “Adv” and the second type was labeled “SG.”
- Embedment depth of headed anchors: The four different embedment depths were 317, 254, 203, and 152.4 mm (12.5, 10, 8, and 6 in.).

The concrete testing specimens were divided into two groups as follows:

- The first group (labeled A) was composed of nine 508 × 533 mm (20 × 21 in.), 355 mm (14 in.) thick concrete blocks. All specimens were reinforced with five 16M (no. 5) bars in the long direction and four 13M (no. 4) bars in the short direction at the top and bottom. Each specimen had a truncated cylindrical shear pocket at the middle that had a 127 mm (5 in.) top diameter and 152 mm (6 in.) bottom diameter. **Figure 5** presents the geometric details of group A.
- The second group (labeled B) was composed of nine 508 × 533 mm (20 × 21 in.), 152 mm (6 in.) thick concrete blocks. All specimens were reinforced with five 16M (no. 5) bars in the long direction and four 13M (no. 4) bars at the top only. Each specimen had a truncated cylindrical shear pocket at the middle that had a 114 mm (4.5 in.) top diameter and 127 mm (5 in.) bottom diameter. **Figure 6** presents the geometric details of group B.

## Material properties

The precast concrete blocks were prepared at a precast concrete manufacturing facility in Morris, Ill., and shipped to Chicago, Ill., for testing. The specimens were cast and cured in optimum conditions at the precast concrete manufacturing facility. The average concrete compressive strength for the blocks was about 62 MPa (9000 psi) for all blocks. The grout material was bought from local suppliers. The grout was mixed and cast using the proportions provided by the supplier. The grout was mixed with 11.33 kg (25 lb) of pea gravel with a maximum aggregate size of 9.5 mm ( $\frac{3}{8}$  in.). The average compressive strength for the grout was about 41.36 MPa

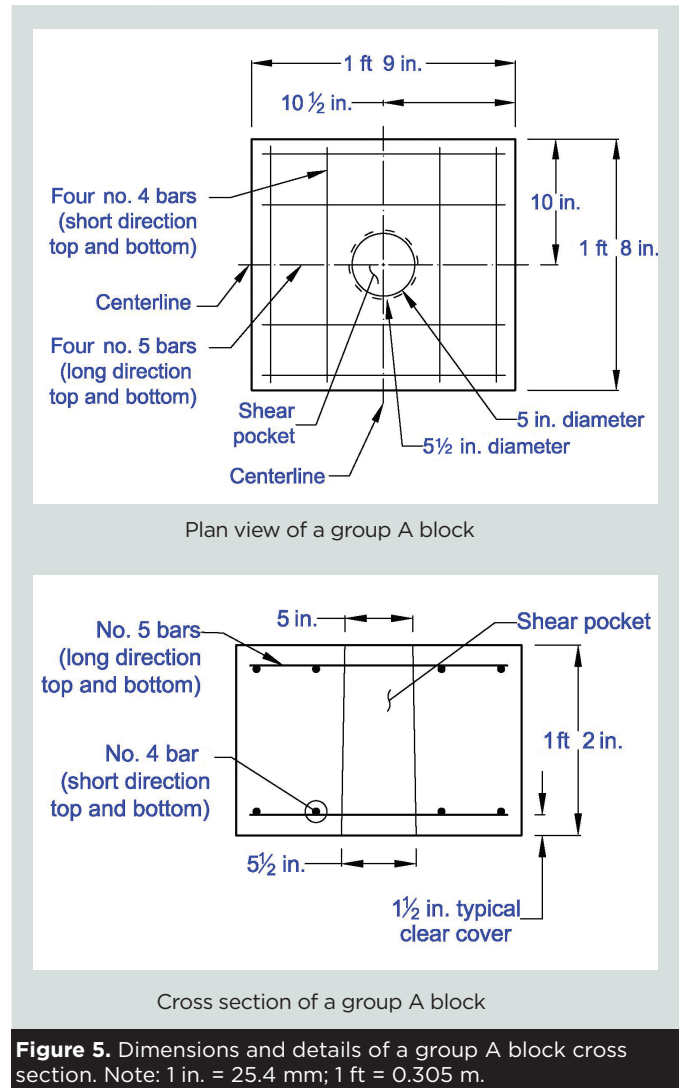


**Figure 5.** Dimensions and details of a group A block cross section. Note: 1 in. = 25.4 mm; 1 ft = 0.305 m.

(6000 psi) for all samples. **Table 3** presents the mixture proportions for the concrete used for the blocks and the two types of the grout. The headed steel anchors were epoxy coated and made from Grade 60 (420 MPa) steel.

## Experimental program

### Testing schedule

**Table 4** presents the testing schedule for all concrete blocks.

**Table 3.** Concrete mixture proportions for precast concrete blocks and grout

Material	Concrete for blocks, kg/m <sup>3</sup>	Adv grout, kg/m <sup>3</sup>	SG grout, kg/m <sup>3</sup>
Sand	785.7	0.0	0.0
Coarse aggregate	905.5	678.5	702.2
Cementitious materials	415.1	1356.8	1404.5
Water	157.7	226.6	191.6
Water-cement ratio	0.38	0.167	0.136
Air content	6.50	n/a	n/a

Note: Adv = commercially available product 1; n/a = not applicable; SG = commercially available product 2. 1 kg/m<sup>3</sup> = 1.69 lb/ycd<sup>3</sup>.

## Specimen preparation

As mentioned, the shear pockets within the concrete blocks were formed at the precast concrete manufacturing facility using conical cylinders wrapped with debonding agent. The debonding agent left traces of grease on the interior face of the shear pockets. Therefore, every shear pocket was sandblasted using black diamond abrasive sand at a pressure of 1.03 MPa (150 psi). After sandblasting, the specimens were cleaned using pressurized air to remove all dust particles remaining from the sandblasting process. Each shear pocket was sealed from the bottom using extruded polystyrene foam and filled with clean water, allowing it to cure for 24 hours before grouting (Fig. 7).

The grout was mixed according to the proportions provided by the manufacturer using a mechanical mixer with rotating blades. Each grout bag (22.67 kg [50 lb]) was dry mixed for 10 minutes to thoroughly mix all the constituents. About ¾ of the water was added to the grout. The remaining water was added later to achieve flowability. The components were mixed for about five minutes. A special frame was designed to align the headed anchors before casting. Each anchor was placed and leveled in the center of the shear pocket at the desired embedment depth. The curing water was drained out of the shear pocket right before grouting. Figure 8 shows the specimen preparation setup.

## Experimental testing

The experimental testing was conducted using an automatic hydraulic machine. The tests were conducted using a controlled strain rate for steel of 1000 µε/min. The testing machine was composed of two hydraulic systems: a fixed system to support the top of the concrete block during testing and a movable system with a loading jaw to apply the load. Each specimen was loaded on the machine, and the steel bar was caught with the loading jaw. Figure 9 shows the experimental setup.

An extensometer with a gauge length of 50.8 mm (2 in.) was used to control the strain rate during testing through a feedback signal. The extensometer was mounted on the headed bar. In addition, a strain gauge and a linear variable displacement transformer (LVDT) (placed in a special fixture) were

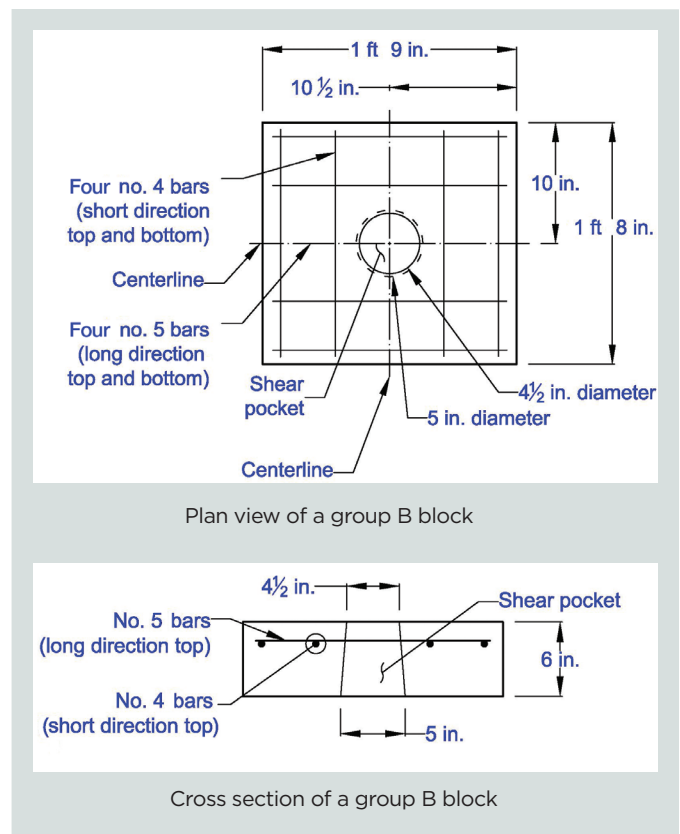


**Figure 6.** Dimensions and details of a group B block cross section. Note: 1 in. = 25.4 mm; 1 ft = 0.305 m.

used to measure the strain in the headed bar as backup readings. The total gauge length of the LVDT fixture was 100 mm (3.93 in.). To measure the relative slip, a hole was drilled at the bottom of the blocks at the centerline of the headed bars and a 25 mm (0.98 in.) LVDT was mounted at the bottom using a specially designed aluminum fixture. Figure 10 shows the typical instrumentation setup.

## Discussion of experimental test results

### Effect of bar size

Figure 11 compares the stress and strain results of the 29M,

**Table 4.** Details of the testing schedule

Quantity	Anchor size and type	Grout type	Specimen	Remarks
2	29M-D	Adv	A#29D-ADV-1 ( $l_d = 318$ mm)*	Block group: A Thickness = 355 mm Reinforcing material: five 16M top and bottom in long direction and four 13M top and bottom in short direction Purpose: test typical thickness of slab with similar reinforcement
		SG	A#29D-SG-2 ( $l_d = 318$ mm)*	
1	25M-D	Adv	A#25D-ADV-1	
1	25M-P	Adv	A#25P-ADV-1	
2	22M-D	Adv	A#22D-ADV-1	
		SG	A#22D-ADV-1	
3	29M-D	Adv	A#29D-ADV-1 ( $l_d = 254$ mm)*	
		Adv	A#29D-ADV-2 ( $l_d = 203$ mm)*	
		Adv	A#29D-ADV-3 ( $l_d = 152$ mm)*	
2	22M-D	SG	B#22D-SG-1	
		SG	B#22D-SG-2	
1	22M -P	SG	B#22P-SG-1	
1	25M-P	SG	B#25P-SG-2	
2	25M-D	SG	B#25D-SG-1	
		SG	B#25D-SG-2	
1	29M-D	SG	B#29D-SG-1	
2	19M-D	SG	B#19D-SG-1	
		SG	B#19D-SG-2	

\* The embedment depths of specimens A#29-D varied to examine the change in the mode of failure associated with changing the embedment depth of the headed anchors.

Note: Adv = commercially available product 1;  $l_d$  = embedment depth; SG = commercially available product 2. 13M = no. 4; 16M = no. 5; 19M = no. 6; 22M = no. 7; 25M = no. 8; 29M = no. 9; 1 mm = 0.0394 in.

25M, and 22M (no. 9, 8, and 7) anchors obtained from the experimental testing. All headed anchors, regardless of bar size, failed by yielding of steel before breakout of concrete. They yielded at a stress around 410 MPa (60 ksi). The postyielding behavior of all the anchors was characterized by strain hardening with an increase in stress. The testing was stopped when the strain in the steel anchor exceeded 40,000  $\mu\epsilon$ .

**Table 5** summarizes the experimental test results for each testing block based on the type of headed anchor. All headed anchors registered a modulus of elasticity of around 200 GPa (29,000 ksi). The anchor bars experienced yielding before concrete breakout. This mode of failure was consistent for all three bar sizes. Concrete blocks cast with 25M (no. 8)-P and 25M (no. 8)-D headed anchors (A-#25D-ADV-1 and A-#25P-ADV-1) did not show significant difference in the overall be-

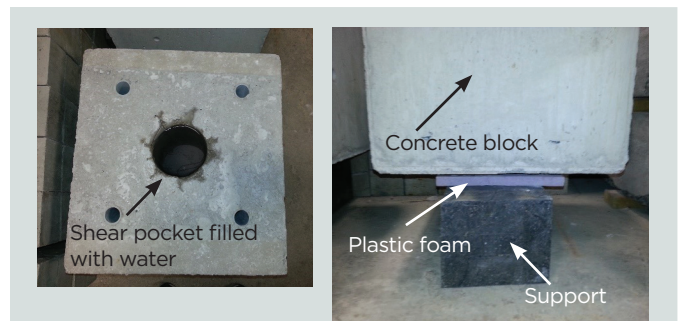


**Figure 7.** Curing setup for test specimens.

havior. Moreover, block cast with grout type “SG” (A-#29D-SG-2 and A-#22D-SG-1) did show any significant difference in performance compared with the specimens cast with grout



type “Adv” (A-#29D-ADV-1 and A-#22D-ADV-1). The ultimate loads listed in Table 5 represent the load registered by each specimen at the time when the test was ended. The tests were stopped when the strain in the anchor bar exceeded 40,000  $\mu\epsilon$  (except for A-#22D-SG-1).

### Effect of bar embedment depth

Figure 12 compares the stress and strain results of the 29M (no. 9) anchors with different embedment depths obtained from the experimental testing. All headed anchors failed by yielding of steel before breakout of concrete for all cases. The stress-versus-strain behavior is consistent for all embedment cases.

According to ACI 318-14 section 25.4.4.2, the development length of epoxy-coated headed anchors in tension shall be  $14.8d_b$  and not less than  $8d_b$  or 152 mm (6 in.), with compressive strength not exceeding 41 MPa (6000 psi). The blocks were tested under axial tensile loading conditions. The conclusions based on this section depend on the quality of grout, good sandblasting, and the fact that the shear pockets solely contain grout material with no confinement reinforcement.

Table 6 summarizes the experimental test results for each testing block based on the embedment depth  $l_d$  of the headed anchor. All headed anchors registered a modulus of elasticity of around 200 GPa (29,000 ksi). As with the different bar sizes, the anchor bars experienced yielding before concrete breakout. This mode of failure was consistent for all embedment depths. The ultimate loads listed in Table 6 represent the load registered by each specimen at the time of ending the test. The tests



Figure 8. Specimen preparation setup.

were stopped when the strain in the anchor bar reached almost 40,000  $\mu\epsilon$  or when fracture in the headed steel bar occurred. This result indicates that yielding in the headed steel bar is expected for all cases including shallow embedment depth.

### Mode of failure

The mode of failure for the 355.6 mm (14 in.) specimens (group A) was characterized by yielding of the headed steel anchor at a stress around 413.68 MPa (60 ksi) followed by strain hardening behavior and necking until fracture of the bar. This result was consistent for all headed anchors with all embedment depths, except for the specimen with an embedment depth  $l_d$  of 152 mm (6 in.). For this specimen, the mode of failure was characterized by yielding of steel anchor at a stress of 413.68 MPa (60 ksi) and breakout of concrete when ultimate load was applied. The cracks extended from the periphery of the grouted shear pocket to the corners of the

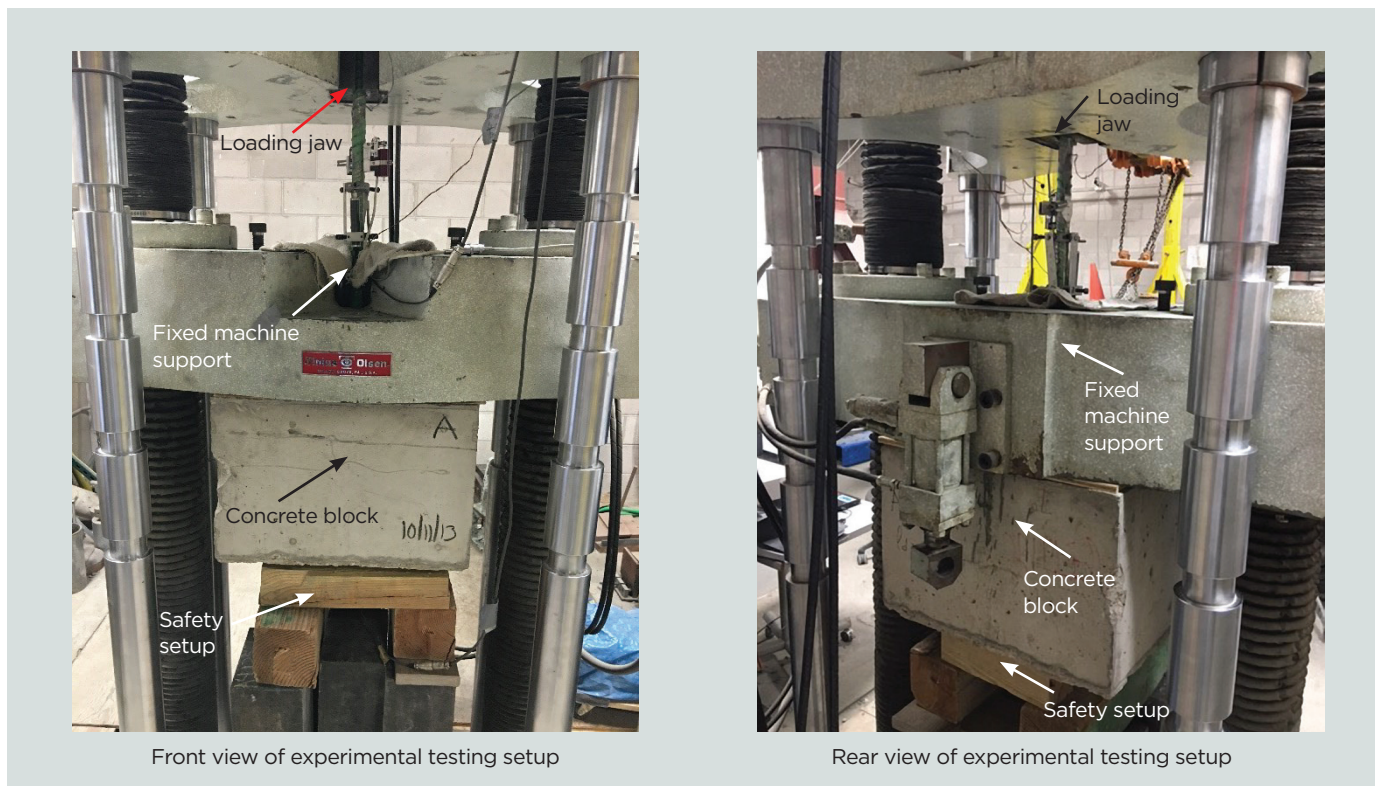
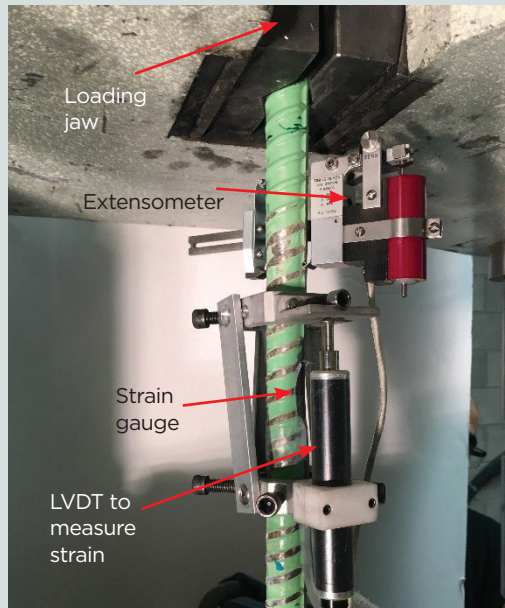
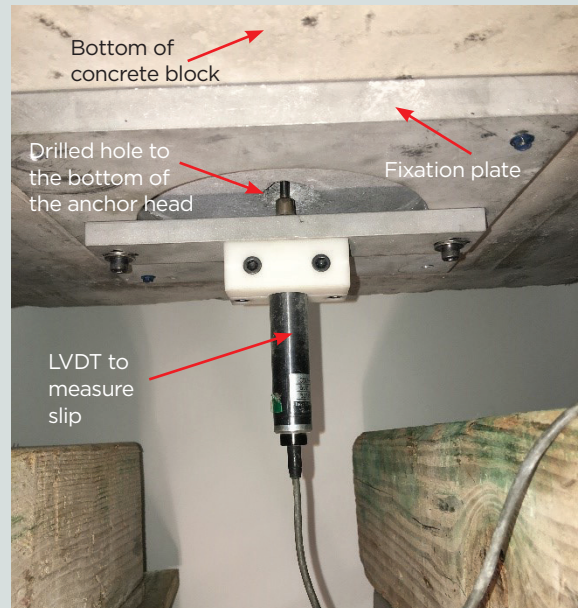


Figure 9. Experimental testing setup for the pull-out blocks.



Instrumentation setup on headed anchor



LVDT at the bottom of block to measure anchor slip

**Figure 10.** Typical instrumentation setup for the testing blocks. Note: LVDT = linear variable displacement transducer.

concrete block. **Figure 13** shows the mode of failure of all blocks in group A.

Group B blocks exhibited the concrete breakout mode of failure before any yielding in the steel anchors. **Figure 14** shows the typical mode of failure for all group B specimens.

Cracks extended from the periphery of the grouted shear pocket to the corners of the concrete block. This mode of failure was attributed to the small block thickness of the group B specimens. This result indicates that a slab thickness of 152 mm (6 in.) is insufficient to obtain full development length of the headed anchors. After propagation of cracks in the concrete, the shear pockets exhibited separation from the concrete block at the bond interface.

## Finite element analysis

A detailed nonlinear finite element model was developed to analyze the pull-out behavior of the headed anchors. The purpose of finite element modeling is to do the following:

- investigate the pull-out behavior of the headed anchors used in the totally prefabricated counterfort retaining wall
- investigate the mode of failure of the anchor-shear pocket system

## Concrete, grout, anchors, and steel reinforcement

Concrete volume was modeled using a specialized element for modeling concrete materials that simulates the crack-

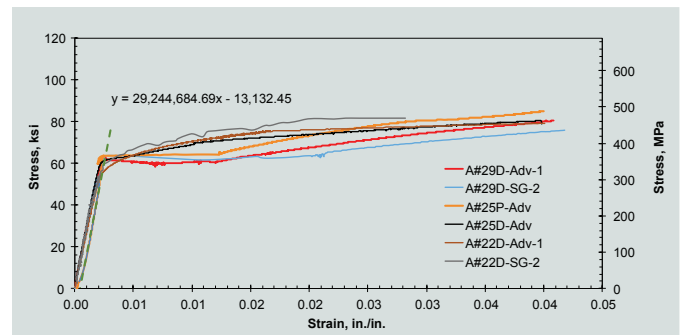


**Figure 11.** Strain-versus-stress results for group A specimens with different anchor sizes.

ing and crushing behaviors of concrete. The simulation of cracking and crushing is based on the Willam and Warnke model, which predicts when concrete will fail. The crushing capability of concrete was ignored in several studies to avoid fictitious crushing.<sup>24–26</sup> A uniaxial multilinear stress-strain curve was obtained from concrete cylinder testing and input to the model to define compressive behavior of concrete. A value of 0.2 was used for Poisson's ratio of concrete. The compressive strength, modulus of rupture, and modulus of elasticity of precast concrete were set to 62.1, 4.9, and 37.23 GPa (9000 psi, 711 psi, and 5400 ksi), respectively. The modulus of rupture and modulus of elasticity of concrete were calculated according to ACI 318-14 Eq. (19.2.3.1) and (19.2.2.1), respectively.

The grout material was modeled separately. The same analytical model was used for the grout, but the material properties were changed. The compressive strength, modulus of rupture, and modulus of elasticity of the grout material were set to

**Table 5.** Experimental test results for group A blocks with different bar sizes

Specimen (embed- ment depth = 318 mm)	Ultimate load, kN	Strain at ultimate load, $\mu\epsilon$	Modulus of elasticity, GPa	Behavior
A-#29D-Adv-1	358.8	40,192	202.71	Yielding in anchor
A-#29D-SG-2	386.5	48,547	201.96	Yielding in anchor
A-#25D-Adv	283.0	39,804	204.62	Yielding in anchor
A-#25P-Adv	351.2	55,110	201.64	Yielding in anchor
A-#22D-Adv-1	214.4	49,009	194.74	Yielding in anchor
A-#22D-SG-2	218.1	23,100	198.30	Yielding in anchor

Note: 1 mm = 0.0394 in.; 1 kN = 0.225 kip; 1 GPa = 145 ksi.

**Table 6.** Experimental test results for headed blocks with different embedment depths

Specimen	Embedment depth $l_d$ , mm	Embedment depth $l_d$ to bar diameter $d_b$ ratio	Ultimate load, kN	Strain at ulti- mate load, $\mu\epsilon$	Modulus of elasticity, GPa	Behavior
A#29D-Adv-1 ( $l_d = 318$ mm)	317.5	11.1	358.7	40,192	202.71	Yielding in anchor
A#29D-SG-2 ( $l_d = 318$ mm)	317.5	11.1	348.1	48,547	201.96	Yielding in anchor
A#29D-Adv ( $l_d = 254$ mm)	254	8.8	365.3	39,992	200.36	Yielding in anchor
A#29D-Adv ( $l_d = 203$ mm)	203.2	7.1	339.2	34,388	197.28	Yielding in anchor
A#29D-Adv ( $l_d = 152$ mm)	152.4	5.3	358.6	39,732	196.96	Yielding in anchor

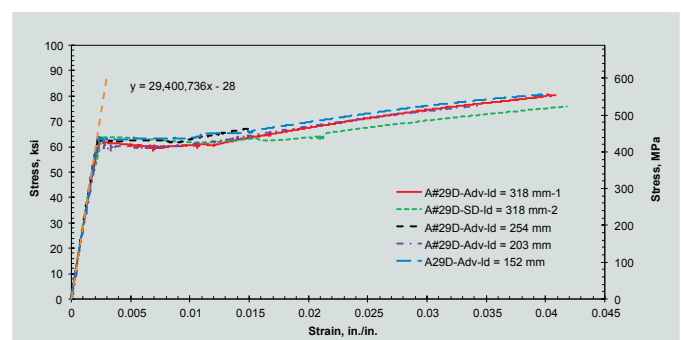
Note: 1 mm = 0.0394 in.; 1 kN = 0.225 kip; 1 GPa = 145 ksi.

41.4 MPa, 4.0 MPa, and 30.33 GPa (6000 psi, 581 psi, and 4400 ksi), respectively.

The headed anchors were modeled using a general-purpose element that can model steel material. It is defined by eight nodes with three translational degrees of freedom (x, y, and z) at each node. This element can provide plasticity capability. The anchors were modeled with a modulus of elasticity of 200 GPa (29,000 ksi) and a Poisson's ratio of 0.3.

Steel reinforcement was modeled using a different specialized element. The steel material was assumed to be bilinear elastic-perfectly plastic that is identical in both tension and compression, with a modulus of elasticity of 200 GPa (29,000 ksi) and Poisson's ratio of 0.3. The interface between the specialized steel and concrete elements are assumed fully bonded. **Table 7** summarizes the material properties for all components used in the finite element analysis.

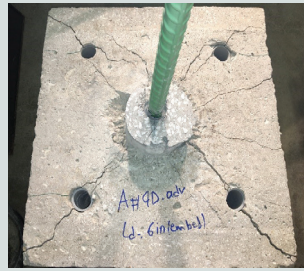
The nonlinear material property for the steel headed anchors was taken from results obtained from experimental testing.

**Figure 12.** Strain-versus-stress results for group A specimens with different embedment depths. Note: 1 in. = 25.4 mm.

The strain versus stress obtained was divided into an ascending linear portion until the yielding point at a strain of 2070  $\mu\epsilon$  and stress of 413.7 MPa (60 ksi), a plateau characterized by a large strain increase (until 10,000  $\mu\epsilon$ ) with a slight increase in stress, and a strain hardening portion with increasing strain and stress. **Figure 15** shows the material model using in the finite element analysis for headed anchors.



Mode of failure of A#9-Adv- $l_d = 12.5$ in.



Mode of failure of A#9-Adv- $l_d = 6$ in.

**Figure 13.** Mode of failure for all group A specimens and for A#9D-Adv with a 6 in. embedment depth. Note: 1 in. = 25.4 mm.

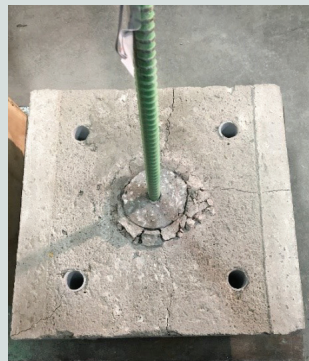


**Figure 14.** Mode of failure of group B blocks with no. 7 and 8 bars (typical failure). Note: no. 7 = 22M; no. 8 = 25M.

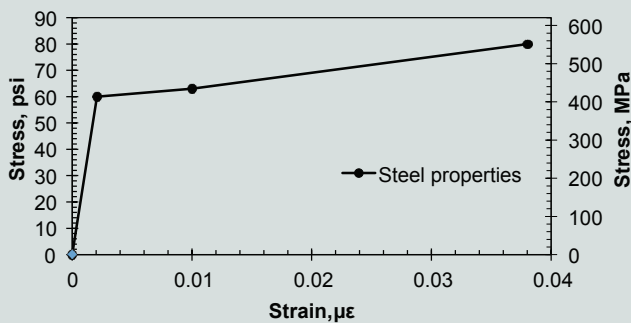


**Figure 15.** Material properties for steel headed anchors used in finite element analysis.

## Loading and boundary conditions

The boundary conditions were set to mimic the actual testing conditions. The top face of the concrete block excluding the grout zone was restrained from translation in the vertical direction. The loading was applied in the form of displacement in the steel anchor. A total displacement of 50.8 mm (2 in.) was assigned to the top nodes of the steel anchor. **Figure 16**

**Table 7.** Material properties for all components used in finite element analysis

Component	Description	Value
Concrete block	Compressive strength of concrete block $f'_c$ , MPa	62.1
	Modulus of rupture of concrete block $f_r$ , MPa	4.9
	Unit weight of concrete $\gamma_c$ , kg/m <sup>3</sup>	2402.8
	Modulus of elasticity of concrete block $E_c$ , GPa	37.23
	Poisson's ratio $\eta_c$	0.2
Grout	Compressive strength of grout material $f'_c$ , MPa	41.4
	Modulus of rupture of grout material $f_r$ , MPa	4.0
	Unit weight of grout $\gamma_g$ , kg/m <sup>3</sup>	2402.8
	Modulus of elasticity of grout material $E_c$ , GPa	30.33
	Poisson's ratio $\eta_c$	0.2
Headed anchors and steel reinforcement	Yield strength of steel $f_y$ , MPa	413.7
	Modulus of elasticity of steel $E_s$ , GPa	200
	Poisson's ratio $\eta_s$	0.3
	Unit weight of steel $\gamma_s$ , kg/m <sup>3</sup>	7849.0

Note: 1 kN = 0.225 kip; 1 MPa = 0.145 ksi; 1 GPa = 145 ksi; 1 kg/m<sup>3</sup> = 1.69 lb/yd<sup>3</sup>.

shows the finite element model and the boundary and loading conditions. To reduce the computation time, one quarter of the mode was modeled and quarter symmetry boundary conditions were applied.

## Analysis and discussion of nonlinear finite element analysis results

The structural behavior and the mode of failure of the headed anchors–shear pocket system is discussed based on the finite element analysis results.

**Behavior of headed anchors** The results obtained from the finite element analysis show that all headed anchors yielded when the tensile stresses reached 413.7 MPa (60 ksi). **Figure 17** shows the strain versus load results obtained from the finite element analysis for the 29M, 25M, and 22M (no. 9, 8, and 7) headed anchors. The 29M headed anchor yielded at a load of 266.9 kN (60,000 lb). In addition, the 25M and 22M headed anchors yielded at loads of 210.84 and 162.8 kN (47,400 and

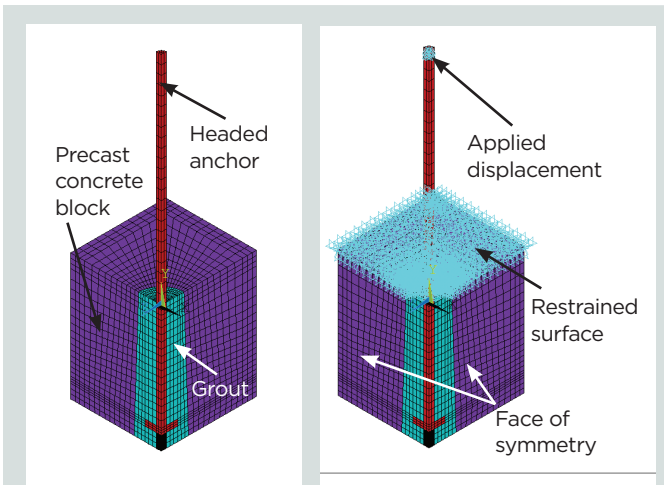


**Figure 16.** Finite element model and boundary conditions.

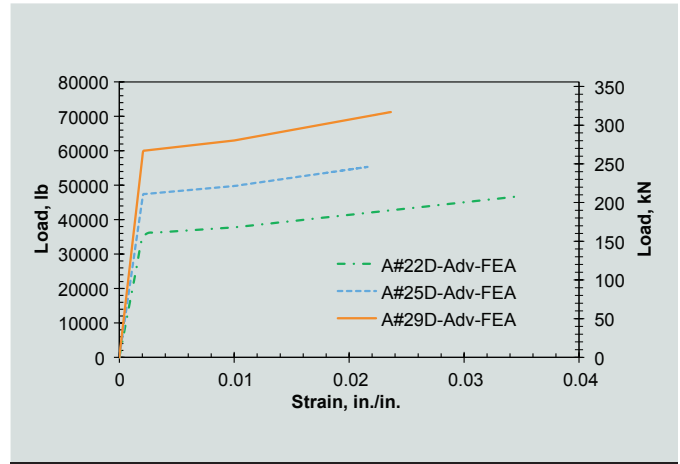


**Figure 17.** Strain versus load results obtained from the finite element analysis using no. 9, 8, and 7 headed anchors. Note: no. 7 = 22M; no. 8 = 25M; no. 9 = 29M; 1 in. = 25.4 mm.

36,000 lb), respectively. The general behavior of the headed anchor depicted that of the assigned material property because the mode of failure of the headed bars was characterized by yielding before major damage in the concrete. Therefore, all headed anchors were characterized by an increasing elastic behavior until reaching the yielding point of 413.7 MPa (60 ksi), followed by a plateau with a slight increase in the stress until reaching a strain of 10,000  $\mu\epsilon$  and followed by strain hardening behavior.

**Behavior of shear pocket** The results obtained from the finite element analysis show that development of minor cracks in the shear pocket after yielding of headed anchors. It was noticed that the cracks propagated in a conical shape at an angle varying from 26 to 42 degrees (**Fig. 18**). This observation is consistent with the ACI 318-14 and the AISC concrete capacity design methods for calculating the breakout capacity of concrete.

### Validation of nonlinear finite element analysis results with experimental results

The results obtained from the finite element analysis were compared with those obtained from the experimental investigation. **Figure 19** shows the strain versus load for all specimens having an embedment depth of 317 mm (12.5 in.) obtained from the experimental test results and the finite element analysis. There is a very good correlation between the experimental testing results and the finite element analysis results. The finite element model predicted both the structural behavior and the mode of failure of the pull-out specimens.

### Comparison with design methods

**Table 8** shows a comparison of the results obtained from the

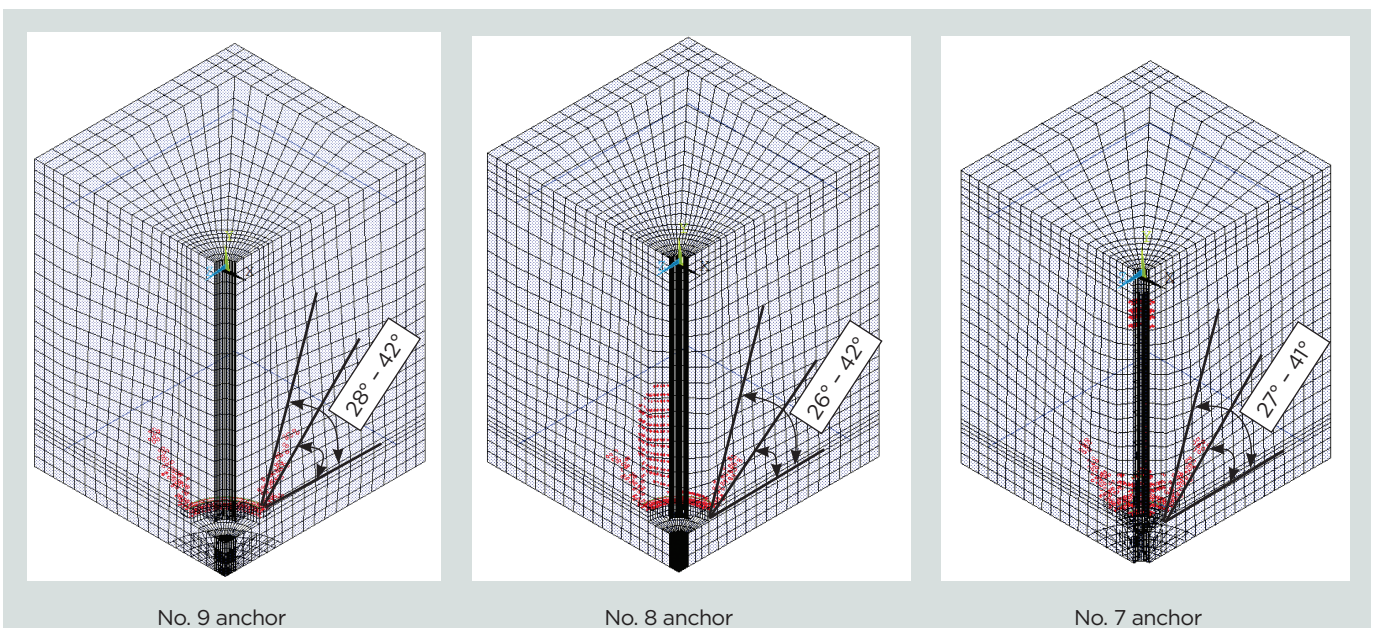


**Figure 18.** Development of cracks in the shear pocket from finite element analysis. Note: no. 7 = 22M; no. 8 = 25M; no. 9 = 29M.

experimental testing, design methods, and studies found in the literature. There is a close correlation between the experimental test results and the AISC *Steel Design Guide 1: Base Plate and Anchor Rod Design* for concentric compressive axial load. The average percentage difference between the experimental result and AISC was about 13.3% for 29M (no. 9) anchors, 1.8% for 25M (no. 8) anchors, and 11.7% for 22M (no. 7) anchors.

The American Society of Civil Engineers' (ASCE's) concrete capacity design method correlated well with the 29M and 25M headed anchors with 317 mm (12.5 in.) embedment lengths. The percentage differences between the experimental test results and the ASCE concrete capacity design method for 29M and 25M anchors were 5.24% and 6.32%, respectively. However, the ASCE concrete capacity design method was found to overestimate the strength of 22M anchors by 36.1%. Moreover, when the embedment length was reduced, the estimated strength using the concrete capacity design method showed very conservative results compared with the experimental testing results to underestimate the strength of the headed anchors.

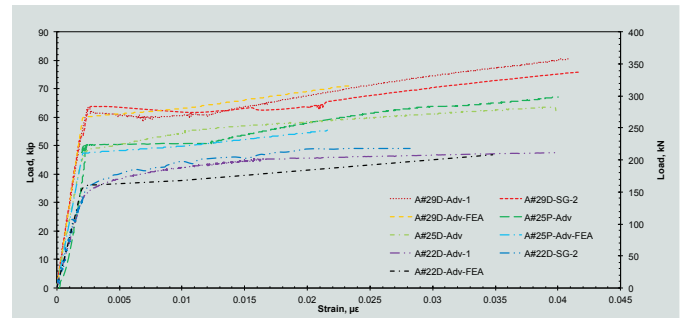


**Figure 19.** Strain versus load for all specimens with a 12.5 in. embedment depth obtained from the experimental test results and the finite element analysis. Note: 1 in. = 25.4 mm.

The studies conducted by Thompson et al.,<sup>27,28</sup> DeVries,<sup>19</sup> and Marchetto<sup>29</sup> at the University of Texas did not correlate well with the experimental test results. The ACI 318-14 concrete breakout strength in tension (section 17.4.2) was found to underestimate the concrete breakout capacity. In fact, this method does not take into account the effect of the size of the headed anchors.

**Table 8.** Comparison of experimental test results, design methods, and studies in literature

Method		Specimen failure load, kN					
		29M $l_d = 317$ mm	29M $l_d = 254$ mm	29M $l_d = 203$ mm	29M $l_d = 152$ mm	25M $l_d = 317$ mm	22M $l_d = 317$ mm
Experimental test results		353.32*	365.20	339.04	358.48	316.98†	216.18‡
AISC guide 1 concentric compressive axial load		408.57	408.57	408.57	408.57	322.90	244.96
AISC guide 1 tensile axial load	Concrete pull-out strength	1153.60	1153.60	1153.60	1153.60	911.75	691.65
	Concrete capacity design	235.00	164.50	114.45	70.86	235.00	235.00
ACI 318-14		102.09	102.09	102.09	102.09	102.09	102.09
DeVries		359.19	359.19	359.19	359.19	290.16	252.93
FHWA/TX-0-1855-1 and FHWA/TX-04/1855-3		298.12	298.12	298.12	298.12	265.03	230.82
Marchetto		290.47	290.47	290.47	290.47	496.73	490.91

\* Averaged between A-#29D-ADV-1 and A-#29D-SG-2.

† Averaged between A-#25D-ADV-1 and A-#25P-ADV-2.

‡ Averaged between A-#22D-ADV-1 and A-#22P-SG-2.

Note: Adv = commercially available product 1;  $l_d$  = embedment depth; SG = commercially available product 2. 22M = no. 7; 25M = no. 8; 29M = no. 9; 1 mm = 0.039 in.; 1 kN = 0.225 kip.

## Conclusion

An experimental study and a nonlinear finite element analysis were performed to examine the overall breakout behavior of headed anchors subjected to tensile loading. Precast concrete blocks (533 × 508 mm [21 × 20 in.]) having a shear pocket identical to those used in the totally prefabricated counterfort retaining wall were prepared, grouted with headed anchors, instrumented, and experimentally tested. The study took into consideration two different block thicknesses (355 and 152 mm [14 and 6 in.]), two IDOT-certified types of headed anchors and types of concrete grout, different bar sizes (22M, 25M, and 29M [no. 7, 8, and 9]), and different embedment depths (317, 254, 203, and 152 mm [12.5, 10, 8, and 6 in.]). The blocks were tested under axial tensile loading conditions. The following conclusions can be drawn:

- Although the experimental test results showed good correlation with the AISC design guide for anchor rods, ACI 318-14 seemed to underestimate the concrete breakout capacity.
- The headed anchor size and the difference in the embedment depth did not affect the failure mode. Specimens with a 152 mm (6 in.) embedment depth failed by yielding of steel anchor and breakout of concrete at ultimate load. However, this only occurred at ultimate load after yielding of the headed anchors. It can safely be assumed in the structural design that the headed anchors will yield before breakout of concrete regardless of the headed anchor size, grout type, and embedment depth of at least 152 mm (6 in.).
- Finite element analysis confirms angle of crack propagation in the shear pocket with the AISC design guide for headed anchors. The angle varied from 26 to 42 degrees.
- The headed anchor size and the difference in the embedment depth did not affect the failure mode. Specimens with a 152 mm (6 in.) embedment depth failed by yielding of steel anchor and breakout of concrete at ultimate load. However, this only occurred at ultimate load after yielding of the headed anchors. It can be safely assumed in the structural design that the headed anchors will yield before breakout of concrete regardless of the headed anchor size, grout type, and embedment depth greater than 152 mm (6 in.) (better to take 254 mm [10 in.] to be on the safe side).
- Based on the results obtained from the experimental testing program and the nonlinear finite element analysis, headed anchors of any size (up to 29M [no. 9]) and any embedment depth (not less than 152 mm [6 in.]) can be safely used in the design of totally prefabricated counterfort retaining walls without the risk of concrete breakout before yielding of steel.

## References

1. Farhat, M., M. Rahman, M. Ibrahim, and M. A. Issa. 2014. "Design, Fabrication, Modeling and Experimental Study of a Totally Precast Concrete Counterfort Retaining Wall System for Highways." In *2014 PCI Convention and National Bridge Conference: Proceedings, September 6–9, 2014, Washington, DC*. Chicago, IL: PCI.
2. Farhat, M., M. Rahman, M. Ibrahim, and M. A. Issa. 2015. "Design Optimization and Modeling of a Totally Precast Concrete Counterfort Retaining Wall System." In *Proceedings of the 16th European Bridge Conference in Edinburgh, UK, 22–25 June 2015*. Edinburgh, UK: ECS Publications.
3. Farhat, M., M. Issa, M. Ibrahim, and M. Rahman. 2017. "Full-Scale Experimental Testing and Finite Element Analysis of a Totally Prefabricated Counterfort Retaining Wall System." *PCI Journal* 62 (3): 72–87.
4. AASHTO (American Association of State Highway and Transportation Officials). 2014. *AASHTO LRFD Bridge Design Specifications*. 7th ed., customary U.S. units. Washington, DC: AASHTO.
5. Farhat, M., and M. A. Issa. 2017. "Fabrication and Construction of Totally Prefabricated Counterfort Retaining Wall System for Highways." *Practice Periodical on Structural Design and Construction* 22 (2). [https://doi.org/10.1061/\(ASCE\)SC.1943-5576.0000316](https://doi.org/10.1061/(ASCE)SC.1943-5576.0000316).
6. Farhat, M., and M. Issa. 2017. "Design Principles of Totally Prefabricated Counterfort Retaining Wall System Compared with Existing Cast-In-Place Structures." *PCI Journal* 62 (5): 89–106.
7. ACI (American Concrete Institute) Committee 318. 2014. *Building Code Requirements for Structural Concrete (ACI 318-14) and Commentary (ACI 318R-14)*. Farmington Hills, MI: ACI.
8. Rodriguez, M., D. Lotze, J. H. Gross, Y.-G. Zhang, R. E. Klingner, and H. L. Graves. 2001. "Dynamic Behavior of Tensile Anchors to Concrete." *ACI Structural Journal* 98 (4): 511–524.
9. Rodriguez, M., Y.-G. Zhang, D. Lotze, H. L. Graves, and R. E. Klingner. 1997. "Dynamic Behaviour of Anchors in Cracked and Uncracked Concrete: A Progress Report." *Nuclear Engineering and Design* 168 (1–3): 23–24.
10. Eligehausen, R., and T. Balogh. 1995. "Behavior of Fasteners Loaded in Tension in Cracked Reinforced Concrete." *ACI Structural Journal* 92 (3): 365–379.
11. Sattler, K. 1962. "Betrachtungen über Neuere Verdübelungen im Verbundbau." *Der Bauingenieur* 37 (1): 1–8.

12. Sattler, K. 1962. "Betrachtungen über Neuere Verdübelungen im Verbundbau." *Der Bauingenieur* 37 (2): 60–67.
13. Nelson Stud Welding. 1966. "Concrete Anchor Test No. 7." Project 802. Lorain, OH: Nelson Division.
14. McMackin, P. J., R. G. Slutter, and J. W. Fisher. 1973. "Headed Steel Anchor under Combined Loading." *Engineering Journal* 10 (2):43–52.
15. Cannon, R. W., E. G. Burdette, and R. R. Funk. 1975. *Anchorage to Concrete*. Report CEB 75-32. Knoxville, TN: Tennessee Valley Authority.
16. Lee, N. H., K. S. Kim, G. C. J. Bang, and K. R. Park. 2007. "Tensile-Headed Anchor with Large Diameter and Deep Embedment in Concrete." *ACI Structural Journal* 104 (4): 479–486.
17. Fuchs, W., R. Eligehausen, and J. Breen. 1995. "Concrete Capacity Design (CCD) Approach for Fastening to Concrete." *ACI Structural Journal* 92 (1): 73–93.
18. Fisher, J. M., and L. A. Kloiber. 2006. *Steel Design Guide 1: Base Plate and Anchor Rod Design*. Chicago, IL: AISC (American Institute of Steel Construction).
19. DeVries, R. A. 1996. "Anchorage of Headed Reinforcement in Concrete." PhD diss., University of Texas at Austin.
20. Bashandy, T. R. 1996. "Application of Headed Bars in Concrete Members." PhD diss., University of Texas at Austin.
21. Delhomme, F., T. Roure, B. Arrieta, and A. Limam. 2016. "Pullout Behavior of Cast-in-Place Headed and Bonded Anchors with Different Embedment Depths." *Materials and Structures* 49 (5): 1843–1859.
22. AFNOR (Association Française de Normalisation). 2009. *Design of Fastenings for Use In Concrete—Part 4-2: Headed Fasteners*. European technical specification XP CEN/TS 1992-4-2. Paris, France: AFNOR.
23. Qian, S., and V. C. Li. 2011. "Headed Anchor/Engineered Cementitious Composites (ECC) Pullout Behavior." *Journal of Advanced Concrete Technology* 9 (3): 339–351.
24. Kachlakev, D., T. Miller, S. Yim, K. Chansawat, and T. Potisuk. 2001. "Finite Element Modeling of Concrete Structures Strengthened with FRP Laminates." Final report. SPR 316/ FHWA-OR-RD-01-XX. Salem, OR: Oregon Department of Transportation Research Group.
25. Zhou S., D. C. Rizos, and M. F. Petrou. 2004. "Effects of Superstructure Flexibility on Strength of Reinforced Concrete Bridge Decks." *Computers & Structures* 82 (1): 13–23.
26. Si, B. J., Z. G. Sun, Q. H. Ai, D. S. Wang, and Q. X. Wang. 2008. "Experiments and Simulation of Flexural-Shear Dominated RC Bridge Piers under Reversed Cyclic Loading." In *The 14th World Conference on Earthquake Engineering Proceedings, Beijing, China, October 12–17, 2008*. Heilongjiang, China: Chinese Association of Earthquake Engineering.
27. Thompson, M. K., J. O. Jirsa, J. E. Breen, and R. E. Klingner. 2002. "Anchorage Behavior of Headed Reinforcement: Literature Review." FHWA/TX-0-1855-1. Austin, TX: Texas Department of Transportation.
28. Thompson, M. K., A. L. Ledesma, J. O. Jirsa, J. E. Breen, and R. E. Klingner. 2003. "Anchorage Behavior of Headed Reinforcement: Part A: Lap Splices, Part B: Design Provisions and Summary." FHWA/TX-04/1855-3. Austin, TX: Texas Department of Transportation.
29. Marchatto, F. 2015. "Use of Headed Reinforcement Bars in Construction." Master's diss., Technical University of Madrid.

## Notation

$A_1$	= loaded area for consideration of bearing strength
$A_2$	= area of the lower base of the largest frustum of a pyramid, cone, or tapered wedge contained wholly
$A_b$	= area of the bar or anchor
$A_{bo}$	= blowout area for corner placement
$A_{bon}$	= basic blowout area for corner placement
$A_{brg}$	= bearing area of the anchor rod head or nut
$A_{brg}$	= net bearing area of the head of stud, anchor bolt, or headed deformed bar
$A_N$	= concrete breakout cone area for group
$A_{N0}$	= concrete breakout cone area for single anchor
$A_{Nc}$	= projected concrete failure area of a single anchor or group of anchors
$A_{Nco}$	= projected concrete failure area of a single anchor for calculation of strength in tension if not limited by edge distance or spacing
$A_{nh}$	= net bearing area of the head (neglecting the bar area)
$A_{se,N}$	= effective cross-sectional area of the anchor bar
$c_1$	= dimension orthogonal to $c_2$



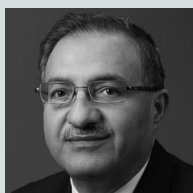
$c_2$	= the minimum of half the center-to-center bar spacing or the least overall cover dimension measured to the center of the bar	$\eta_s$	= Poisson's ratio of steel
$d_b$	= diameter of the bar or anchor	$\lambda_a$	= modification factor to reflect the reduced mechanical properties of lightweight concrete in certain concrete anchorage applications
$E_c$	= modulus of elasticity of concrete or grout material	$\phi$	= strength reduction factor
$E_s$	= modulus of elasticity of steel	$\psi_3$	= factor used to modify pull-out strength of anchors based on presence or absence of cracks in concrete
$f'_c$	= concrete compressive strength	$\psi_4$	= factor used to modify concrete breakout strength of a single anchor based on presence or absence of cracks in concrete
$f_r$	= modulus of rupture of concrete	$\Psi$	= radial disturbance factor
$f_{s,head}$	= bearing strength of headed anchors	$\Psi_{c,N}$	= factor used to modify tensile strength of anchors based on presence or absence of cracks in concrete
$f_{ua}$	= specified tensile strength of anchor steel	$\Psi_{c,P}$	= factor used to modify pull-out strength of anchors based on presence or absence of cracks in concrete
$f_y$	= yield strength of steel	$\Psi_{cp,N}$	= factor used to modify tensile strength of post-installed anchors intended for use in uncracked concrete without supplementary reinforcement to account for the splitting tensile stresses due to installation
$f_{ya}$	= specified yield strength of anchor steel	$\Psi_{ed,N}$	= factor used to modify tensile strength of anchors based on proximity to edges of concrete member
$h_{ef}$	= effective embedment depth of anchor		
$k_c$	= coefficient for basic concrete breakout strength in tension		
$l_d$	= embedment depth		
$n_{5\%}$	= 5% exclusion factor		
$N_b$	= basic concrete (cracked) breakout strength of a single anchor in tension		
$N_{cb}$	= nominal concrete (uncracked) breakout strength of a single anchor		
$N_{cgb}$	= nominal concrete (uncracked) breakout strength of a single anchor calculated by the concrete capacity design method		
$N_p$	= nominal pull-out strength		
$N_{pn}$	= pull-out strength of headed anchors		
$N_{sa}$	= nominal strength of the anchor in tension		
$P$	= nominal pull-out strength		
$P_u$	= ultimate pull-out strength		
$\gamma_c$	= unit weight of concrete		
$\gamma_g$	= unit weight of grout		
$\gamma_s$	= unit weight of steel		
$\eta_c$	= Poisson's ratio of concrete		

## About the authors



Maen Farhat is a graduate research assistant and PhD candidate in the Department of Civil and Materials Engineering at the University of Illinois at Chicago. His current research interests are accelerated bridge construction, precast

concrete, and recycled high-density polyethylene crossties. Farhat is also involved in various research topics, including concrete materials with an emphasis on concrete durability and sustainability, advanced composites, and ultra-high-performance concrete.



Mohsen Issa, PhD, FACI, FASCE, PE, SE, is a professor of structural and materials engineering in the Department of Civil and Materials Engineering at the University of Illinois at Chicago. His research interests include structural

buildings and bridges, development of experimental and analytical techniques for monitoring and rating existing highway bridges, high-density polyethylene recycled plastic materials and high-density polyethylene crossties, advanced composites, concrete durability, accelerated bridge construction techniques, and sustainability.



Bruno F. J. Prado is an undergraduate student in civil engineering in the College of Engineering, Architecture, and Geography at the Federal University of Mato Grosso do Sul in Campo Grande, Brazil. He was an undergraduate research intern in the Department

of Civil and Materials Engineering at the University of Illinois at Chicago through the Science Without Borders exchange program.

## Abstract

The pull-out behavior of headed anchors used in a totally prefabricated precast concrete counterfort retaining wall system was examined experimentally and analytically using nonlinear finite element analysis. Precast concrete blocks ( $533 \times 508$  mm [ $21 \times 20$  in.]) having a truncated shear pocket identical to those used in the totally prefabricated counterfort retaining wall were prepared, grouted with headed anchors, instrumented, and experimentally tested. The study includes the following parameters: two block thicknesses of 355 and 152 mm (14 and 6 in.); two types of headed anchors and two types of concrete grout certified by the Illinois Department of Transportation; bar sizes 19M, 22M, 25M, and 29M (no. 6, 7, 8, and 9); and embedment depths of 317, 254, 203, and 152 mm (12.5, 10, 8, and 6 in.).

The blocks were tested under axial tensile loading conditions. The structural behavior of the pull-out specimens was characterized by the fracture of steel anchors, regardless of their size and embedment depth. Concrete breakout was witnessed in 355 mm (14 in.) thick concrete specimens made with 29M headed anchors and 152 mm (6 in.) embedment depth only when the specimen was tested to ultimate. The experimental test results were verified using finite element analysis and compared with design methods and other studies in the literature. The results showed close correlation with the American Institute of Steel Construction's guidelines.

## Keywords

Embedment depth, finite element analysis, grout, headed anchor, pull-out.

## Review policy

This paper was reviewed in accordance with the Precast/Prestressed Concrete Institute's peer-review process.

## Reader comments

Please address any reader comments to *PCI Journal* editor-in-chief Emily Lorenz at [elorenz@pci.org](mailto:elorenz@pci.org) or Precast/Prestressed Concrete Institute, c/o *PCI Journal*, 200 W. Adams St., Suite 2100, Chicago, IL 60606.